International Journal of Advances in Engineering and Management (IJAEM)
Volume 6, Issue 07 July 2024, pp: 433-441www.ijaem.net ISSN: 2395-5252

# Spatiotemporal Analysis of Land Use and Land Cover Types and Their Impacts on Land Surface Temperature of Abia State, Nigeria

Ukanwa, S. O., Ejikeme, J. O and Uwandu, I.G.
*Department of Surveying and Geoinformatics, NnamdiAzikiwe University, Awka, Anambra State*

Date of Submission: 10-07-2024 Date of Acceptance: 20-07-2024

**ABSTRACT**
Rapid urbanization results to an increase in impervious layers which therefore increases the land surface temperature massively. This study is aimed at performed a spatiotemporal analysis of land surface temperature and its impact on land use/land cover types in Abia State of Nigeria. Lansat 8 OLI imageries of 2013, 2018 and 2023 were used for data analysis to retrieve the land surface temperature (LST) and the land use/ land cover (LULC) types. The methodology adopted by study for LST retrieval was the Single Channel Algorithm (SCA) and for classifying the LULC, the Supervised Classification using Maximum Likelihood Classifier (MLC) algorithm was used. The ArcGIS 10.8 was used to classify LULC types and estimate the LST. The findings indicate that LULC significantly affects LST values due to the biophysical characteristics of the land surfaces. Vegetation and water bodies lower surface temperatures, suggesting that integrating vegetation within urban areas at regular intervals can help maintain a cooler urban thermal environment. Moderate LST differences were observed between bare lands and vegetation, as well as between barren land and built-up areas, while the smallest LST differences were noted between water bodies and vegetation. The study also found that the highest LSTs are typically observed in cities such as Aba and Umuahia within the state. The study will have a positive health impact in the study area and help policies makers and relevant agencies in making an information decision and policies based on the findings from the study.

**KEYWORDS:**Land Use/Land Cover (LULC) classification, LST, SCA and SCA

## I. INTRODUCTION

Land use and land cover (LULC) changes are significant indicators of environmental transformation. These changes, driven by natural processes and anthropogenic activities, profoundly impact ecological balance, climate, and human livelihoods.The majority of the rise in surface temperature is due to the conversion of vegetated areas into impervious surfaces, as well as the transformation of vegetated and wetland areas into agricultural land or bare wasteland (Mallick et al., 2008). Rapid urbanization results to an increase in impervious layers which therefore increases the land surface temperature massively (Hossain et al., 2020). The land surface temperature can be considered an effective measure for predicting radiation budgets for heat balance, it can be an important indicator in understanding the interactions that occur between the environment and humans in urban environments and also an important factor controlling the physical and biological processes of land systems (Tan et al., 2010). Furthermore, the increase in land surface temperature effects the urban heat island (UHI) phenomena, having a significant influence on biodiversity's primary function, local and regional climate (Luck and Wu, 2002).

As a result of the spatiotemporal landuse/ landcover variations, this alters on the pattern of a variety of land surfaces of spatial landscapes and it is therefore critical to ascertain landuse/ landcover changes at appropriate scales using accurate time series data. Studies have shown that land cover changes influence the surface temperature due to the different heat capacity of soils associated to a given amount of solar radiation (Fonsekaet al., 2019).

International Journal of Advances in Engineering and Management (IJAEM)
Volume 6, Issue 07 July 2024, pp: 433-441www.ijaem.net ISSN: 2395-5252

Abia State, located in southeastern Nigeria, has experienced considerable LULC changes over the past few decades. This study aims to analyze the spatiotemporal dynamics of these changes and assess their impacts on land surface temperature (LST), a critical parameter influencing local climate and environmental conditions.

## II. MATERIALS AND METHODS

### 2.1 Study Area

Abia State is located in the southeastern region of Nigeria. Abia State lies between latitudes 4°40'N and 6°14'N and longitudes 7°10'E and 8°00'E. The state covers an area of approximately 6,320 square kilometers. It is bordered by Imo State to the west, Enugu and Ebonyi States to the north, Cross River State to the east, AkwaIbom State to the southeast, and Rivers State to the south. The terrain is predominantly low-lying with some hilly areas in the northern parts.The climate of Abia State is characterized by two distinct seasons: the rainy season, which lasts from April to October, and the dry season, from November to March. The state experiences high humidity and significant rainfall during the rainy season, while the dry season is marked by lower humidity and less precipitation. The average annual temperature ranges between 24°C and 28°C.Abia State is part of the tropical rainforest zone, with dense vegetation comprising both primary and secondary forests. The state also has areas of derived savanna, particularly in regions that have experienced deforestation and agricultural activities. Wetlands are also present, especially along the riverine areas. Fig. 1 shows the map of the study area.

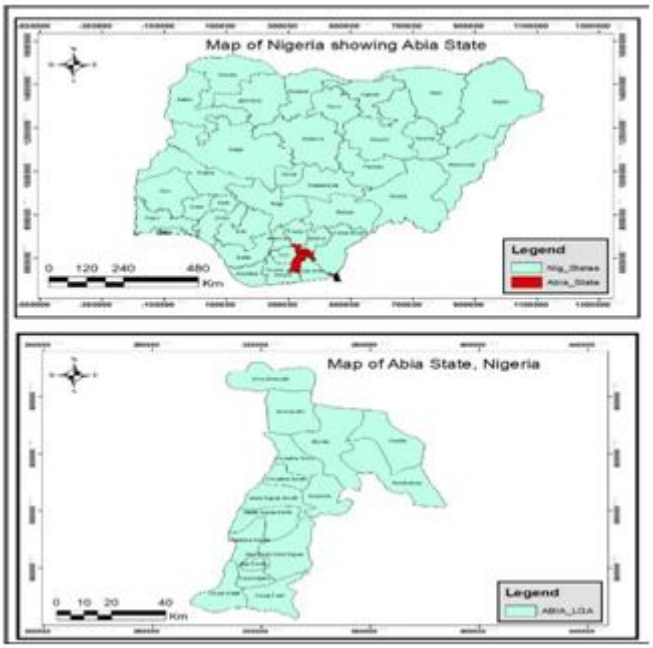


**Fig 1: Map of the study area**

### 2.2 Materials

In this study, Table 1. shows the different datasets used for this study and their sources.

| S/N | Data | Acquisition Date | Scale | Source |
|---|---|---|---|---|
| 1 | Landsat 8 OLI_TIRS | 2013-07-21 | 30m ™ | U.S. Geological Survey(USGS) |
| 2 | Landsat 8 OLI_TIRS | 2018-06-17 | 30m ™ | U.S. Geological Survey(USGS) |
| 3 | Landsat 8 OLI_TIRS | 2023-07-26 | 30m ™ | U.S. Geological Survey (USGS) |
| 4 | Google Earth Data | | | Google Earth |
| 5 | Administrative Map ofAbia State | | | OSGOF |

International Journal of Advances in Engineering and Management (IJAEM)
Volume 6, Issue 07 July 2024, pp: 433-441www.ijaem.net ISSN: 2395-5252

**2.3 Methods**

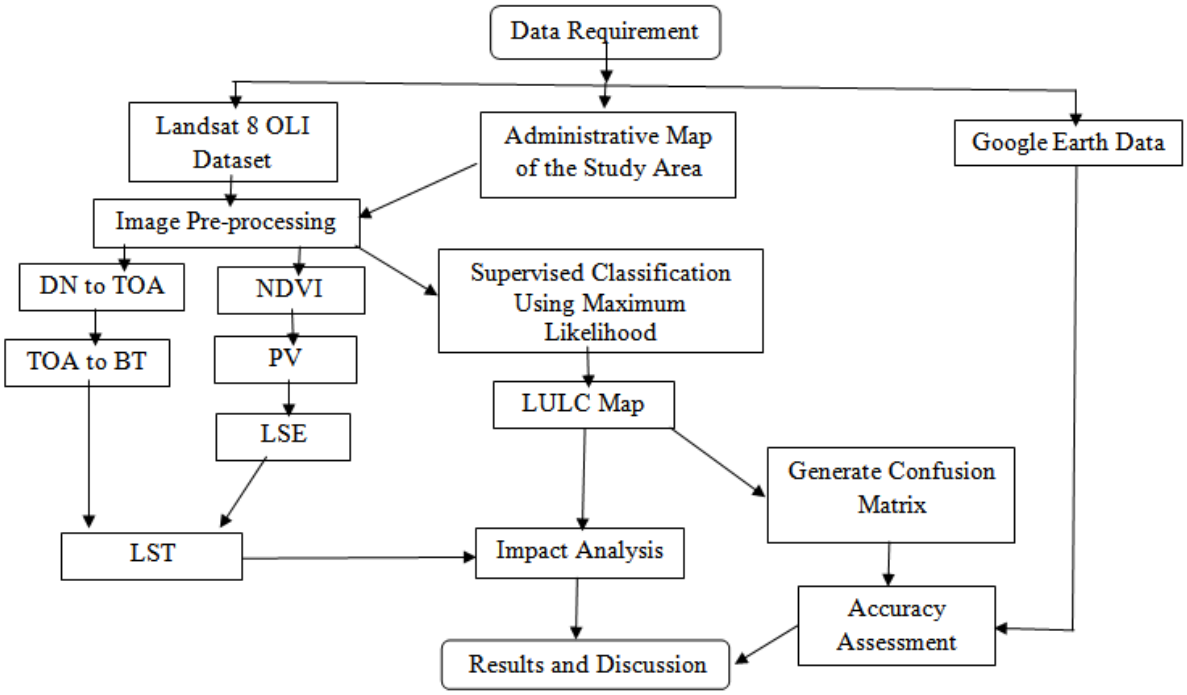


**Fig 2: Flowchart of methodology adopted by the study**

**Source: The Author**

**2.4 Image Processing and Classification**

The Landsat 8 OLI imageries were used for LULC classificationusingthe supervised classification method. With the prior knowledge of the study area, the training samples for the supervised classification operation were created. Training samples were created in the satellite imagery by drawing polygons, which was placed in an area of interest (AoI) layer. The signature file was created and the maximum likelihood algorithm was used as the supervised classification classifier. The maximum likelihood classifier (MLC) have over the years been widely used for the classification of medium-resolution satellite imagery like the Landsat 8 OLI imagery. A statistical approach is used by the maximum likelihood classifier for pattern recognition and the assumption is that the statistics for each class in each image band have a normal distribution. The implementation of the algorithm is simple and widely used for varying remote sensing applications as it computes the probability of any given pixel, belonging to each class and assigns it to the class (Ahmad and Quegan, 2012).

Table 2.0 shows the different land use and land cover types for the study.

**Table 2: Description of land cover types for the study.**

| S/N | LULC Category | Description |
|---|---|---|
| 1. | Built-up lands | All residential, commercial, and industrial areas, village settlements, and transportation infrastructure |
| 2 | Vegetation covers | Trees, shrub land and semi-mature vegetation, deciduous, coniferous, and mixed forests, palms, orchids, herbs, gardens, and grasslands |
| 3 | Bare land | Naturally occurring soils with no vegetation cover or above-ground cover within the study area. |
| 4 | Water bodies | River, permanent open water, lakes, ponds, canals, and Reservoirs |

International Journal of Advances in Engineering and Management (IJAEM)
Volume 6, Issue 07 July 2024, pp: 433-441www.ijaem.net ISSN: 2395-5252

**2.5Accuracy Assessment**

To determine the reliability and accuracy of the land use and land cover, this study performed the accuracy assessment using the confusion/ error matrix.According to Hasmadiet al., (2009) accuracy assessment of image classification is an important step in determining the reliability of the results obtained from the classification process. Anderson (1997) noted that at least a minimum of 85% interpretation accuracy should be attained in the identification of land cover classes from remotely sensed data. To calculate for the producer accuracy, user accuracy, and overall accuracy Equation (1) was used.

$$Kappa = \frac{P(a) - P(e)}{1 - P(e)} \quad \ldots\ldots\ldots\ldots (2)$$

$$\text{Overall Accuracy (\%)} = \frac{\text{Total Number of correctly classified samples}}{\text{Total number of samples}} \times 100 \quad \ldots(1)$$

Where,
P(a) is the relative observed agreement
P(e) is the hypothetical probability of chance agreement.

**2.6 Land Surface Temperature Retrieval**

Retrieving land surface temperature from thermal bands of a satellite image is not a straightforward task as there are different processes to undertake. The Landsat 8 OLI imageries was used for LST retrieval using the Single Channel Algorithm (SCA). The following procedures were be used:

**2.6.1 Conversion of Digital Numbers to Top-of-Atmosphere (TOA)**

To calculate the LST, the first process is the conversion of spectral radiance digital numbers (DNs) stored in the thermal data of the Landsat sensor and provides a manner of representing pixels that have not yet been calibrated and converted into radiance units. The following equation is used:

$$L\lambda = ML \times Q_{cal} + AL - O_i \quad \ldots\ldots\ldots\ldots\ldots\ldots\ldots\ldots\ldots\ldots\ldots\ldots\ldots\ldots (3)$$

Where,
Lλ is the TOA spectral radiance in Watts/ ($m^2$.sr. µm)
ML is the band-specific multiplying rescale factor in the metadata
AL is the band-specific additive rescaling factor in the metadata
$Q_{cal}$ is the calibrated and quantized pixel values (DN),
$O_i$ represents the offsets supplied by USGS for the TIRS band calibration (Sobrinoet al., 2004).

**2.6.2 Conversion of Radiance to Brightness Temperature (BT)**

The converted TOA is required to be converted to brightness temperature (BT) by removing the effects of the atmosphere in the thermal region (Barsiet al., 2005). This is calculated with an assumption of unity emissivity and using pre-launch calibration constants. The radiant temperature is revised by adding absolute zero (approx. −273.15 ◦C). To achieve this, the thermal constants provided in the metadata file are used as well as the following equation:

$$BT = \frac{K2}{Ln(K1/L\lambda + 1)} - 273.15 \quad \ldots\ldots\ldots\ldots\ldots (4)$$

Where,
Lλ is the TOA spectral radiance
K1 is the Band 10 constant band-specific thermal conversions from the metadata
K2 is the Band 11 constant band-specific thermal conversions from the metadata.

**2.6.3 Calculating of Normalized Difference Vegetative Index (NDVI)**

The NDVI is an important component in calculation of LST as factors such as proportionate vegetative index (PV) and land surface emisivity are all dependent on it. To calculate the NDVI, the following equation was used:

$$NDVI = \frac{NIR - Red}{NIR + Red} \quad \ldots\ldots\ldots (5)$$

Where,
NIR is near-infrared band
Red is red band.
For this study, Landsat 8 OLI data was utilized and the near infrared is Band 5 while Red is Band 4.

International Journal of Advances in Engineering and Management (IJAEM)
Volume 6, Issue 07 July 2024, pp: 433-441www.ijaem.net ISSN: 2395-5252

**2.6.4 Calculating Proportionate Vegetation Index (PV)**

According to Sobrinoet al., (2004), the PV is the vegetation proportion viewed by derived using the following equation:

$$PV = \frac{NDV - NDVI\ min}{NDVI\ max - NDVI\ min} \quad \ldots\ldots (6)$$

Where,
NDVI max is for vegetation
NDVI min is for bare ground

**2.6.5 Calculating Land Surface Emissivity (LSE)**

The land surface emissivity is a proportionality factor that scales blackbody radiance (Planck's law) to predict emitted radiance and represents the efficiency of transmitting thermal energy across the surface into the atmosphere and it's an important factor in calculating the LST (Darren et al., 2020).

The LSE can be calculated using the following equation

$LSE = \varepsilon S \times (1 - Pv) + (\varepsilon V \times Pv)$ .....(7)

Where,
εV and εS are the vegetation and soil emissivity, respectively
Pv is the proportionate vegetation index

For this study, the emissivity constants of Band 10 of Landsat 8 OLI was used which are εS = 0.971 and εV = 0.987 respectively.

**2.6.6 Calculating Land Surface Temperature (LST)**

$$LST = \frac{BT}{1 + \left(\frac{BT}{\rho}\right) Ln\ LSE} \quad \ldots (8)$$

Where,
BT is at-sensor brightness temperature,
ρ = h × c/σ = 1.438 × 10-2 mK, and it is further converted to $\mu m$ units
Furthermore, $h$ is Planck's constant (6.626 × 10-34 Js), $\sigma$ is the Boltzmann constant (1.38 × 10−23 J/K) and $c$ is the velocity of light (2.998 × 108 m/s) (Avdan and Jovanovska, 2016).

**2.7LULC Types Impacts Analysis on LST**

The LULC and LST results were integrated to determine the impacts of LULC types on LST of Abia State. This was carried in ArcGIS through data integration process.

## III. RESULTS AND DISCUSSION

**3.1 Classification Results**

The results of the LULC Analysis using supervised classification method from 2013 to 2023 are presented in Fig 3 and Table 3 respectively.

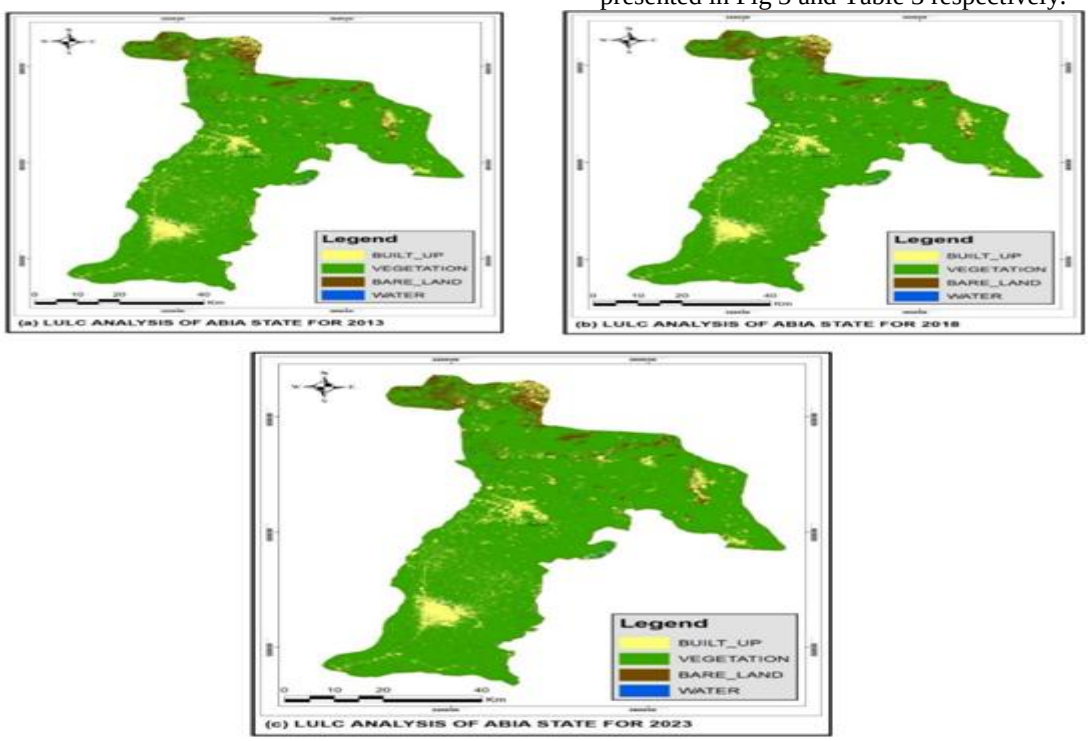


**Figure 3: Classified Maps of (a) 2013, (b) 2018, and (c) 2023**

International Journal of Advances in Engineering and Management (IJAEM)
Volume 6, Issue 07 July 2024, pp: 433-441www.ijaem.net ISSN: 2395-5252

| Year | Built-up Areas (Sq.Km) | Vegetation (Sq.Km) | Bare Lands (Sq.Km) | Water Bodies (Sq.Km) |
|---|---|---|---|---|
| 2013 | 779.882 (12.34%) | 5102.726 (80.74%) | 314.733 (4.98%) | 122.607 (1.94%) |
| 2018 | 882.265 (13.96%) | 5059.118 (80.05%) | 260.382 (4.12%) | 118.183 (1.87%) |
| 2023 | 977.064 (15.46%) | 4975.063 (78.72%) | 248.374 (3.93%) | 119.447 (1.89%) |

The results as shown in Fig 3 and Table 3, in 2013, vegetation occupied the highest landuse area (80.74%), followed by built-up areas with 779.882Sq. Km (12.34%), bare lands with 314.733 Sq. Km (4.98%) and water bodies with 314.733 Sq. Km (4.98%). In 2018, vegetation occupied the highest area with 5059.118Sq. Km (80.05%), followed by built-up areaswith 882.265 Sq. Km (13.96%),the bare lands and water bodies occupies 260.382 Sq. Km (4.12%)and 118.183 Sq. Km (1.87%) respectively. In 2023, vegetation occupied the highest area with 4975.063Sq. Km (78.72%), followed by built-up areaswith 977.064 Sq. Km (15.46%),the bare lands and water bodies occupies 248.374 Sq. Km (3.93%) and 119.447 Sq. Km (1.89%) respectively.

### 3.2 Classification Accuracy Assessment

The confusion/ error matrix were used to determine the reliability and accuracy of the land use and land cover analysis for the study. Theresultsoftheaccuracyassessmentwerepresentedin Tables4, 5and6 respectively.

**Table 4: Classification Accuracy Assessment for 2013**

| Landuse Classes | Built- up | Vegetation | Bare Lands | Water bodies | Total | User's Acc. (%) |
|---|---|---|---|---|---|---|
| Built- up | 52 | 0 | 3 | 0 | 55 | 94.55 |
| Vegetation | 0 | 56 | 0 | 4 | 60 | 93.33 |
| Bare Lands | 4 | 0 | 51 | 0 | 55 | 92.73 |
| Water bodies | 0 | 2 | 0 | 62 | 64 | 96.88 |
| **Total** | 56 | 58 | 54 | 68 | 234 | |
| Producer's Acc. (%) | 92.86 | 96.55 | 94.44 | 91.18 | | |
| Overall Acc. (%) | 94.44 | | | | | |
| Kappa Coefficient | 0.94 | | | | | |

**Table 5: Classification Accuracy Assessment for 2018**

| Landuse Classes | Built- up | Vegetation | Bare Lands | Water bodies | Total | User's Acc. (%) |
|---|---|---|---|---|---|---|
| Built- up | 64 | 0 | 4 | 0 | 68 | 94.12 |
| Vegetation | 0 | 52 | 0 | 2 | 54 | 96.30 |
| Bare Lands | 2 | 0 | 52 | 0 | 54 | 96.30 |
| Water bodies | 0 | 2 | 0 | 55 | 57 | 96.49 |
| **Total** | 66 | 54 | 56 | 57 | 233 | |
| Producer's Acc. (%) | 96.97 | 96.29 | 92.86 | 96.49 | | |
| Overall Acc. (%) | 95.71 | | | | | |
| Kappa Coefficient | 0.96 | | | | | |

International Journal of Advances in Engineering and Management (IJAEM)
Volume 6, Issue 07 July 2024, pp: 433-441www.ijaem.net ISSN: 2395-5252

**Table 6: Classification Accuracy Assessment for 2023**

| Landuse Classes | Built-up | Vegetation | Bare Lands | Water bodies | Total | User's Acc. (%) |
|---|---|---|---|---|---|---|
| Built- up | 57 | 3 | 0 | 0 | 60 | 95.00 |
| Vegetation | 2 | 52 | 0 | 0 | 54 | 96.30 |
| Bare Lands | 1 | 0 | 53 | 0 | 54 | 98.15 |
| Water bodies | 0 | 2 | 0 | 53 | 55 | 96.36 |
| **Total** | 60 | 57 | 53 | 53 | 223 | |
| Producer's Acc. (%) | 95.00 | 91.23 | 100 | 100 | | |
| Overall Acc. (%) | 96.41 | | | | | |
| Kappa Coefficient | 0.96 | | | | | |

### 3.3 Land Surface Temperature (LST) Results

To retrieve the LST, the Single Channel Algorithm (SCA) was employed. The Landsat 8 OLI imageries of the study were used and using the Raster Calculator Tools in the ArcGIS software package, the LST were retrieved successfully. The results are presented in Fig. 4.

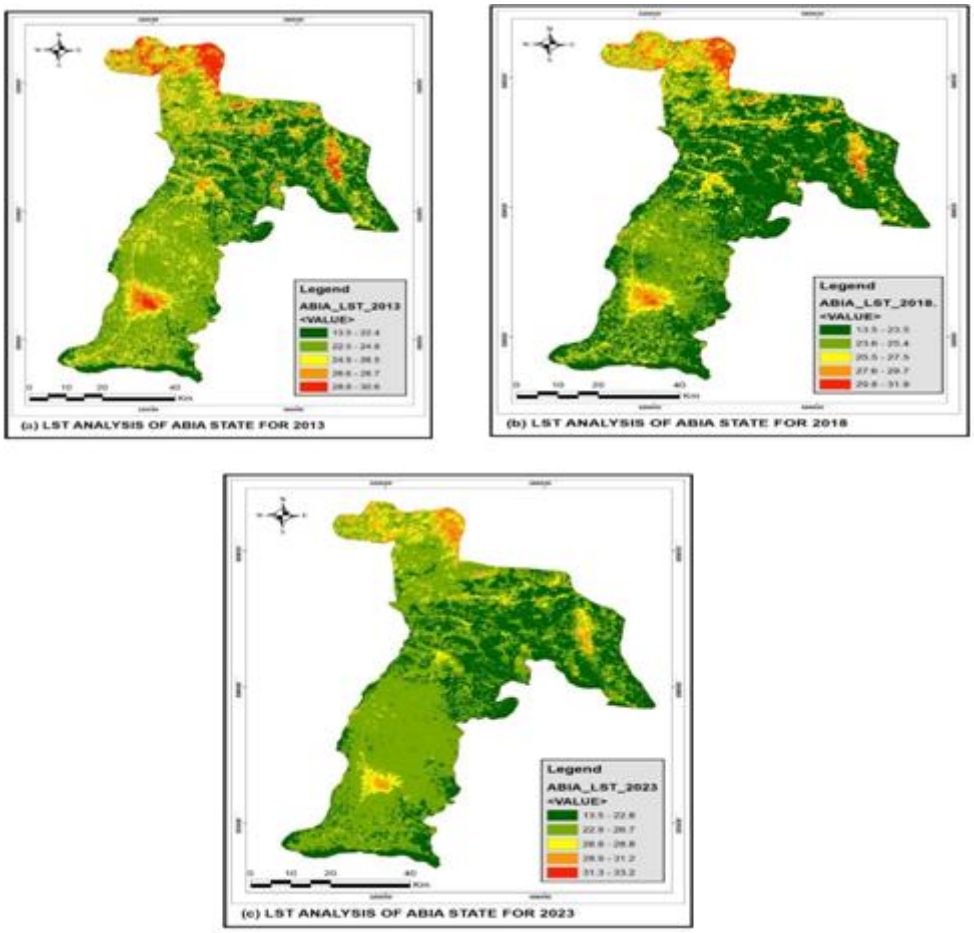


**Figure 4: LST Maps of (a) 2013, (b) 2018, and (c) 2023**

International Journal of Advances in Engineering and Management (IJAEM)
Volume 6, Issue 07 July 2024, pp: 433-441www.ijaem.net ISSN: 2395-5252

The results as shown in Fig 4, in 2013 it was observed that the LST range is from 13.5◦C to 30.6◦C. The lowest LST was 13.5◦C while the highest LST was 30.6◦C while in 2018, the LST range is from 13.5◦C to 31.8◦C. The lowest LST was 13.5◦C while the highest LST was 31.8◦C. and in 2024, the LST range is from 13.5◦C to 33.2◦C. The lowest LST was 13.5◦C while the highest LST was 33.2◦C.

### 3.4 Impact of LULC Types on LST Results

The different LULC types were analyzed to determine their various impacts on LST. The results of the analysis were presented in Table 7.

**Table 7: Impact of LULC Types on LST of Abia State from 2013 to 2023**

| Year | Built-up LST | Vegetation LST | Bare Land LST | Water LST |
|---|---|---|---|---|
| 2013 | 12.34% | 82.74% | 2.98% | 1.94% |
| | 24.9◦C-30.6◦C | 22.5◦C-24.8◦C | 24.9◦C-26.5◦C | 13.5◦C-22.4◦C |
| 2018 | 13.96% | 82.05% | 2.12% | 1.87% |
| | 25.5◦C-29.7◦C | 23.6◦C-25.4◦C | 25.5◦C-27.5◦C | 13.5◦C-23.5◦C |
| 2023 | 15.46% | 80.72% | 1.93% | 1.89% |
| | 26.8◦C-33.2◦C | 22.9◦C-31.2◦C | 26.8◦C-28.8◦C | 13.5◦C-22.8◦C |

From the results in Table 7, in 2013 it was observed that the highest LST range occurred in built-up areas with an average LST ranges of 24.9◦C -30.6◦C while the second highest LST range occurred in bare lands with an LST range of 24.9◦C-26.5◦C, the third highest LST range occurred in vegetation with an LST range of 22.5◦C-24.8◦C and the lowest was water with an LST range of 13.5◦C-22.4◦C. In 2018, it was also observed that the highest LST range occurred in built-up areas with an average LST ranges of 25.5◦C-29.7◦C while the second highest LST range occurred in bare lands with an LST range of 25.5◦C-27.5◦C, the third highest LST range occurred in vegetation with an LST range of 23.6◦C-25.4◦C and the lowest was water with an LST range of 13.5◦C-23.5◦C. Furthermore, it was observed in 2023 that the highest LST range occurred in built-up areas with an average LST ranges of 26.8◦C-33.2◦C while the second highest LST range occurred in bare lands with an LST range of 26.8◦C-28.8◦C, the third highest LST range occurred in vegetation with an LST range of 22.9◦C-31.2◦C and the lowest was water with an LST range of 13.5◦C-22.8◦C.

## IV. CONCLUSION

This study investigated the relationship between Land Use Land Cover (LULC) types and their impact on Land Surface Temperature (LST) in Abia State of Nigeria. The findings indicate that LULC significantly affects LST values due to the biophysical characteristics of the land surfaces. Vegetation and water bodies lower surface temperatures, suggesting that integrating vegetation within urban areas at regular intervals can help maintain a cooler urban thermal environment. Moderate LST differences were observed between bare lands and vegetation, as well as between barren land and built-up areas, while the smallest LST differences were noted between water bodies and vegetation. It was further observed from the study that the highest LSTs are typically observed in cities such as Aba and Umuahia within the state.
From the findings made by the study, the following are recommended:

i. For further research and monitoring should be carried out to ensure sustainable development in Abia State of Nigeria
ii. Establishment of green spaces and greeneries should be encouraged to reduce the high LST in built-up and urban centers.
iii. A sustainable state developmental plan to control anthropogenic activities, including farming and grazing activities.

## REFERENCES

[1]. Anderson, J.R.(1997). Land use classification schemes used in selected recent geographic applications of remote sensing, Photogrammetric Engineering, 37 (4) 379–387.
[2]. Avdan, U., andJovanovska, G. (2016). Algorithm for Automated Mapping of Land Surface Temperature Using LANDSAT 8 Satellite Data. Journal of Sensors.
[3]. Barsi, J. A., Schott, J. R., Palluconi, F. D., and Hook, S. J. (2005). Validation of a web-based Atmospheric correction tool for single thermal band instruments (Conference session). Proceedings SPIE, 58820 E, Bellingham, WA, p. 7.
[4]. Darren, H. J. A., Mohd, H. I. and Farrah, M. M. (2020).Land Use/Land Cover Changes and the Relationship with Land

Surface Temperature Using Landsat and MODIS Imageries in Cameron Highlands, Malaysia. Land 2020

[5]. Fonseka, H.P.U., Zhang, H., Sun, Y., Su, H., Lin, H., and Lin, Y. (2019). Urbanization and its impacts on land surface temperature in Colombo metropolitan area, Sri Lanka, from 1988 to 2016. Remote Sensing, 11 (8, 957), 18 pp

[6]. Hasmadi, M.,Pakhriazad, H.Z. andShahrin, M.F. (2009). Evaluating supervised and unsupervised techniques for land cover mapping using remote sensing data, Malaysian Journal of Social Space, 5 (1) 1–10

[7]. Hossain, M.S., Arshad, M., Qian, L., Kächele, H., Khan, I., Islam, M.D.I, Mahboob, M.G., 2020. Climate change impacts on farmland value in Bangladesh. Ecological Indication. 112,106181.

[8]. Luck, M., Wu, J., 2002. A gradient analysis of urban landscape pattern: a case study from the Phoenix metropolitan region, Arizona, USA. Landscape Ecology, 17, 327–339.

[9]. Mallick, J., Kant, Y., & Bharat, B. (2008). Estimation of land surface temperature over Delhi using Landsat-7 ETM+. Journal of Indian Geophysical Union, 131-140.

[10]. Sobrino, J.A., Munoz, J.C.J. and Leonardo, P. (2004). Land surface temperature retrieval from LANDSAT TM 5. Remote Sensing of Environment, 434 – 440

[11]. Tan, K.C., San Lim, H., MatJafri, M.Z. and Abdullah, K. (2010). Landsat data to evaluate urban expansion and determine land use/land cover changes in Penang Island, Malaysia. Environmental Earth Science. 60, 1509–1521.